

A Dimensional Study of Disk Galaxies

X. Hernandez¹, B. Cervantes-Sodi¹

¹ *Instituto de Astronomía, Universidad Nacional Autónoma de México, A.P. 70-264, 04510 México, D.F.*

23 September 2017

ABSTRACT

We present a highly simplified model of the dynamical structure of a disk galaxy where only two parameters fully determine the solution, mass and angular momentum. We show through simple physical scalings that once the mass has been fixed, the angular momentum parameter λ is expected to regulate such critical galactic disk properties as colour, thickness of the disk and disk to bulge ratio. It is hence expected to be the determinant physical ingredient resulting in a given Hubble type. A simple analytic estimate of λ for an observed system is provided. An explicit comparison of the distribution of several galactic parameters against both Hubble type and λ is performed using observed galaxies. Both such distributions exhibit highly similar characteristics for all galactic properties studied, suggesting λ as a physically motivated classification parameter for disk galaxies.

Key words: galaxies: fundamental parameters – galaxies: general – galaxies: structure

1 INTRODUCTION

The first thing an astronomer wants to know about a galaxy is its morphological type, typically expressed through the Hubble classification scheme, introduced about 80 years ago (Hubble 1926, 1936). Some modifications have been introduced to the details of plan over the years (e.g. de Vaucouleurs 1959, Sandage 1961, Kormendy 1979), although the basics have remained relatively unchanged. The continued usage of the Hubble classification owes its success to the fact that on hearing the Hubble entry of a galaxy, one immediately forms an image of the type of galaxy that is being talked about. A wide variety of physical features of galaxies show good monotonic correlations with Hubble type, despite the presence of significant overlap and dispersion. To mention only a few, total magnitudes decrease towards later types (e.g. Ellis et al 2005) and colours become bluer while gas fractions diminish from early to late types (e.g. Roberts & Haynes 1994). Bulge magnitudes and bulge to disk ratios decrease (e.g. Pahre et al. 2004) and disks become thinner (e.g. de Grijs 1998, Kregel et al. 2002) in going to later types, while the relevance and structure of spiral arms also show marked trends, with decreasing pitch angles, prominence and coherence when one reaches the earlier Hubble types (e.g. Ma 2002, Grosbol 2004). Even the functional shape of galactic bulges correlates with types, e.g. Graham (2001).

However, galactic type classification schemes also suffer from several shortcomings. First, the several diagnostics which enter into the assignment of the type, appearance of

the spiral pattern, bulge to disk ratios, colour, etc., do so in a fundamentally subjective manner e.g. Adams & Woolley (1994). One has to take the images to an expert who will somehow integrate various aspects of the galaxy in question to arrive at the type parameter. That different authors generally agree, together with the correlations between type and various galactic parameters is indicative of a solid physical substrate to galaxy classification schemes, the particular nature of which however, has remained elusive. Second, type parameters are essentially qualitative (e.g. Lotz et al. 2004), which make it difficult to relate type to definitive quantitative aspects of a galactic system, and bring into question the validity of any statistical mathematical analysis performed on galactic populations based on type.

Finally, as has been recognized by many authors, the type given to a galaxy is highly dependent on the information one has regarding the system. This stems from the inputs that determine the galactic type, the relevance of the bulge, typically redder than the disk, means that when observing at longer rest frame bands galaxies shift to earlier types, an effect compounded with the high wavelength sensitivity of the bright HII regions which define the structure and morphology of the spiral arms (e.g. Kuchinsky et al. 2000, Grosbol et al. 2004). This last series of effects is of particular concern when attempting to compare galactic morphologies and types at low and high redshifts, for example, Labbe et al. (2003) have shown that when observing the Hubble Deep Field galaxies in more usual rest frame bands, many of the reported highly disturbed merger morphologies sometimes go away, to reveal essentially standard

disks. Similarly, projection effects become important, as the structure of the arm pattern completely disappears in edge-on disks, eliminating one of the diagnostics relevant to the assignment of type.

In summary, certain discomfort sometimes appears regarding the use of morphological type as the principal tool for galaxy classification, in connection to it being somewhat subjective, intrinsically qualitative, and relative to projection and observation wavelength effects.

Several attempts at improving on these problems have appeared over the years, for example, extensive work has been done in constructing an objective spectral classification scheme for galaxies. These works have concentrated sometimes on the shape of the continuum (e.g. Connolly 1995), others on the relevance of spectral emission and absorption features, as in Zaritsky (1995). These approaches essentially quantify properties of the underlying stellar populations, mainly yielding an objective description of the relative importance of old and young components. The good correlations observed between spectral classifications and Hubble type, indicate that indeed the status of a galaxies stellar population varies monotonically along the Hubble sequence, although it might be a consequence of a more fundamental dynamical/structural physics determining type, and not the defining causal determinant of type itself. A difficulty in applying schemes of the above type massively will of course remain, in connection to the very telescope-time intensive nature of spectroscopy, which increases with the level of detail required e.g. in going from average shapes of the continuum to the details of spectral lines.

A recent related development is the work of Park & Choi (2005) who have showed that the colour-colour gradient plane is split into regions corresponding to distinct galactic types. This last is particularly useful for large samples of galaxies, indeed, it was developed and tested using the Sloan Digital Sky Survey. Again, the physical origin of this separation by types appears to be a characterization of the average age and locality of the star formation history of a galaxy, which in turn would have to be traced back to some more fundamental dynamical/formation physics behind type.

A different approach has been the use of neural networks which are trained to reproduce the subjective process through which experts integrate features of a galaxies image to determine its type. This has the advantage of furnishing a software which can automatically assign galactic types, without the direct intervention of a person e.g. Adams & Wooley (1994), Naim (1997). However, one is left with a black box, the workings of which are difficult to decipher or translate into the physical parameters of a galaxy.

A further line of approach was introduced by Abraham et al. (1994, 1996), who introduced the concentration index C of a galaxies image as a ratio of two radii, fixed as enclosing two given percentages of the total light of the system, at any given wavelength. This approximately corresponds to a bulge to disk ratio, and was shown to correlate well with typical Hubble types. The scheme was extended by Schade et al. (1995) to include an objective measure of the asymmetry of the projected image, through the A index, essentially the quotient of the residual of the images light after a 180 degree rotation of it has been subtracted, to the total light. This last is particularly sensitive to the effects of mergers and interacting systems, but not very relevant

in telling apart the different classes of generally highly 180-rotationally symmetric isolated galaxies along the Hubble sequence. The last component of this image classification scheme is the S clumpiness index introduced by Takamiya (1999) and Conselice (2003), a similar dimensionless index quantifying the degree of small scale structure in an image, similar to the ratio of small scale to large scale power in a polynomial decomposition of the image e.g. (Kelly & McKay 2004). This approach essentially tackles the careful, objective, statistical description of an image through the introduction of the dimensionless parameters expected to be the most representative of the problem. Other variants have appeared, for example Lotz et al. (2004) define two different statistical descriptions of the distribution of light on the sky, and show that this allows an adequate automatic assignment of a galaxies classical Hubble type.

The above methods however, remain somewhat sensitive to projection and wavelength effects, but more seriously, do not include any explicit information of the dynamics of the problem. Certainly, the ability to deduce a galaxies Hubble type from its CAS or other careful objective, dimensionless characterization of its image, suggests these factors vary monotonically along the Hubble sequence. Again, it is not evident how the structural physics of the problem result in a given point in CAS space.

Monotonic trends with Hubble type suggest that after having fixed the mass, there might exist one other parameter whose variation gives rise to the Hubble sequence. Many approaches to galaxy formation and evolution have appeared over the years, generally reaching the conclusion that it is the angular momentum of a galactic system what determines its main characteristics. Some example of which are: Sandage et al. (1970), Brosche (1973), van der Kruit (1987), Fall & Efstathiou (1980), Flores et al. (1993), Firmani et al. (1996), Dalcanton et al. (1997), van den Bosch (1998), Hernandez & Gilmore (1998), Avila-Reese et al. (1998), Zhang & Wyse (2000), Ferguson & Clarke (2001), Silk (2001), Bell (2002), Kregel et al. (2005).

A second problem is what determines the angular momentum of a galaxy at any given time, with older modelings taking this value as a fundamental parameter fixed by initial conditions in the remote past, and more recent CMD cosmological simulations deducing this value as a consequence of the tidal fields of surrounding matter, in combination with the formation history of a halo, with merger events and gas cooling being fundamental to a determination of the sometimes fluctuating value of a galactic systems angular momentum e.g. the cosmological N-body studies of Warren et al. (1992), Cole & Lacey (1996), Lemson & Kauffmann (1999), Steinmetz & Navarro (1999) and Navarro & Steinmetz (2002) or the analytical work of Catelan & Theuns (1996). Whatever the origin or evolution of this parameter, once the mass of a galaxy has been chosen, theoretical studies have typically identified the angular momentum of the system as the principal determinant of a galaxies type. We will therefore focus our attention on this parameter.

Many different models of the structure and evolution of a disk galaxy exist, with varying degrees of detail and including diverse physical aspects of the problem e.g., besides from the above references, including a more explicit cosmological formation scenario, Frenk et al. (1985), Frenk et al. (1988), White et al. (1991), Mo et al. (1998), Somerville &

Primack (1999), Maller et al. (2002) and Klypin et al (2002), to mention only but a representative few. Here we present the simplest possible physical treatment of the problem, not in an attempt to reproduce or understand the details of a disk galaxy, but rather to obtain a first order approximation which might capture the monotonic trends nicely followed by the Hubble sequence. We present a highly simplistic physical modeling of a disk galaxy which allows to estimate its angular momentum parameter λ (Peebles 1969) from readily obtainable structural characteristics.

The layout of our paper is as follows: section 2 presents the physics of the dimensional analysis of disk galaxies, leading to an observational estimate of the λ parameter for any real galaxy. This parameter is then calculated for a large sample of galaxies in section 3, where we also explore the trends followed by different observed galactic properties with λ , and compare with the equivalent trends seen for the Hubble classification. In section 4 we compare our estimated λ parameter for several simulated galaxies from various authors, and present a discussion of our results and conclusions.

2 THEORETICAL FRAMEWORK

As discussed in the introduction, the good monotonic trends followed by a variety of galactic properties along the Hubble sequence reflect not only the usefulness of it, but also suggest that to first order, a disk galaxy can be described by only two parameters, total mass, and some other physical parameter varying monotonically along the Hubble sequence. As mentioned in the introduction, extensive theoretical work leads to the angular momentum as a natural choice for this parameter.

Having chosen the angular momentum as our second parameter we now construct a simple physical model for a galaxy which allows to estimate this parameter directly from observed galactic properties.

In the interest of capturing the most essential physics of the problem, the model we shall develop will be the simplest one could possibly propose, little more than a dimensional analysis of the problem.

2.1 Estimating λ from observations

We shall model only two galactic components, the first one a disk having a surface mass density $\Sigma(r)$ satisfying:

$$\Sigma(r) = \Sigma_0 e^{-r/R_d}, \quad (1)$$

Where r is a radial coordinate and Σ_0 and R_d are two constants which are allowed to vary from galaxy to galaxy. The total disk mass is now:

$$M_d = 2\pi\Sigma_0 R_d^2. \quad (2)$$

The second component will be a fixed dark matter halo having an isothermal $\rho(r)$ density profile, and responsible for establishing a rigorously flat rotation curve V_d throughout the entire galaxy, an approximation sometimes used in simple galactic evolution models e.g. Naab & Ostriker (2005), such that

$$\rho(r) = \frac{1}{4\pi G} \left(\frac{V_d}{r} \right)^2, \quad (3)$$

and a halo mass profile $M(r) \propto r$. Since the total mass of the disk is finite, we define the disk mass fraction as $F = M_d/M_H$. Requiring a finite total halo mass, M_H , will now imply a truncation radius for the dark halo, R_H given by the equation:

$$M_H = \int_0^{R_H} \frac{V_d^2}{G} dr \Rightarrow \quad (4)$$

$$R_H = \frac{M_H G}{V_d^2}.$$

The disk mass fraction F is expected to be of order 1/10 or smaller (e.g. Flores et al. 1993, Hernandez & Gilmore 1998), hence, we shall use global parameters for the entire system indistinctly from halo parameters, consistent with having ignored disk self gravity in eq(3).

It will be convenient to refer not to the total angular momentum L , but to the dimensionless angular momentum parameter

$$\lambda = \frac{L |E|^{1/2}}{GM^{5/2}} \quad (5)$$

where E is the total energy of the configuration and G is Newton's gravitational constant. λ in fact gives the ratio of the actual angular momentum of the system to its maximum possible break-up value, $\lambda = 1$ is hence an upper limit.

We must now express λ in terms of structural galactic parameters readily accessible to observations. First we assume that the total potential energy of the galaxy is dominated by that of the halo, and that this is a virialized gravitational structure, which allows to replace E in the above equation for $W/2$, one half the gravitational potential energy of the halo, given by:

$$W = -4\pi G \int_0^{R_H} \rho(r)M(r)r dr \quad (6)$$

use of equation (3) yields:

$$W = -V_d^2 M_H. \quad (7)$$

Assuming that the specific angular momenta of disk and halo are equal, $l_d = l_H$, as would be the case for an initially well mixed protogalactic state, and generally assumed in galactic formation models e.g. Fall & Efstathiou (1980), Mo et al. (1998).

The specific angular momentum of the disk, following the assumption of a rigorously flat rotation curve and eq(1), will now be $l_d = 2V_d R_d$. We can now replace L for $M_H l_d$. Introducing this last result together with eq(7) into eq(5) yields:

$$\lambda = \frac{2^{1/2} V_d^2 R_d}{GM_H} \quad (8)$$

Finally, we can replace M_H for M_d/F , and introduce a disk Tully-Fisher relation:

$$M_d = A_{TF} V_d^{3.5} \quad (9)$$

into eq(8) to yield:

$$\lambda = \left(\frac{2^{1/2} F}{A_{TF}} \right) \frac{R_d}{G V_d^{3/2}} \quad (10)$$

The existence of a general baryonic Tully-Fisher between the total baryonic component and V_d of the type used here, rather than a specific Tully-Fisher relation involving total magnitude in any particular band, is supported by recent studies, in general in agreement with the 3.5 exponent we assume (e.g. Gurovich et al. 2004 or Kregel et al. 2005 who find 3.33 ± 0.37). All that remains is to choose numeric values for F and A_{TF} , to obtain an estimate of the spin parameter of an observed galaxy in terms of structural parameters readily accessible to observations, R_d and V_d .

Taking the Milky Way as a representative example, we can use a total baryonic mass of $1 \times 10^{11} M_\odot$ and $M_H = 2.5 \times 10^{12} M_\odot$ (where the estimate of the baryonic mass includes all such components, disk, bulge, stellar halo etc., e.g. Wilkinson & Evans 1999, Hernandez et al. 2001) as suitable estimates to obtain $F = 1/25$. For a rotation velocity of $V_d = 220 \text{ km/s}$, the above numbers imply $A_{TF} = 633 M_\odot (\text{km/s})^{-3.5}$, this in turn allows to express eq(10) as:

$$\lambda = 21.8 \frac{R_d / \text{kpc}}{(V_d / \text{km s}^{-1})^{3/2}}, \quad (11)$$

which is the final result of this sub-section. The above equation allows a direct estimate of λ , a dimensionless numerical parameter with a clear physical interpretation for any observed galaxy, with no degree of subjectivity and little sensitivity to orientation effects. The only ambiguity which remains is the definition of the wavelength at which R_d is measured. Recently de Grijs (1998) and Yoachim & Dalcanton (2005) and have measured significant variations in R_d with wavelength. In the spirit of obtaining global mass distribution parameters, it is clear that observations in the r-band or near IR are required for the measure of R_d necessary in eq(11). Also, given the Tully-Fisher relation, it is clear that V_d in eq(11) can be replaced for total magnitude on a given band, for cases where the rotation velocity is not available. It is clear from its derivation that equation (11) is only an approximate way of inferring the λ parameter of an observed galaxy, intended as an objective and quantitative improvement on current classification schemes, and not as a detailed measurement of the angular momentum of a real galaxy. If one intended a more careful measurement of λ , a full dynamical modeling of the rotation curve and bulge and disk matter distribution would be required, of the type found in e.g. Tonini et al. (2005).

For the Galactic values used above, equation (11) yields $\lambda_{MW} = 0.0234$, in excellent agreement with recent estimates of this parameter, e.g. through a detailed modeling of the Milky Way within a CDM framework Hernandez et al. (2001) find $\lambda_{MW} = 0.02$.

2.2 Expected scalings with λ

We now study the expected scaling between λ and other observables of a disk galaxy, for example colour, gas fraction, star formation activity, degree of flatness of the disk and bulge to disk ratios. The main ingredient will be the Toomre parameter,

$$Q(r) = \frac{\kappa(r)\sigma(r)}{\pi G \Sigma(r)}, \quad (12)$$

where $\kappa(r)$ is the epicyclic frequency at a given radius, and $\sigma(r)$ is the velocity dispersion and $\Sigma(r)$ the disk surface density of any given galactic disk component. This parameter measures the degree of internal gravitational stability of the disk, with $\kappa(r)$ accounting for the disruptive shears induced by the differential rotation, $\sigma(r)$ modeling the thermal pressure of a component, both in competition with $\Sigma(r)G$, the self gravity of the disk. Values of $Q \leq 1$ are interpreted as leading to gravitational instability in a 'cold' disk. In the interest of simplicity of the description, and bearing in mind that the angular velocity and the epicyclic frequency are within a factor of order unity of each other, e.g. in a flat rotation curve, $\kappa(r) = \sqrt{2}\Omega(r)$, we shall replace $\kappa(r)$ in eq(12) with $\Omega(r) = V_d/r$, the angular velocity of the disk.

The star formation processes in the disk have often been thought of as forming a self regulated cycle. The gas in regions where $Q < 1$ is gravitationally unstable, this leads to collapse and the triggering of star formation processes, which in turn result in significantly energetic processes. The above include radiative heating, the propagation of ionization fronts, shock waves and in general an efficient turbulent heating of the gas media, raising σ locally to values resulting in $Q > 1$. This restores the gravitational stability of the disk and shuts off the star formation processes. On timescales longer than the few $\times 10$ million years of massive stellar lifetimes, an equilibrium is expected where star formation proceeds at a rate equal to that of gas turbulent dissipation, at time averaged values of $Q \sim 1$. Examples of the above can be found in Dopita & Ryder (1994), Koeppen et al. (1995), Silk (2001).

For example, Silk (2001) uses ideas of this type to derive the local volume density of star formation $\dot{\rho}_{sf}$ as:

$$\dot{\rho}_{sf} = \Omega \rho_g \sigma_g, \quad (13)$$

Where volume densities will be given by $\rho = \Sigma/h$, h the disk scale height. Employing the Toomre criterion at $Q = 1$ to rewrite the gas velocity dispersion in terms of the gas surface density, equation (13) may be written as follows:

$$\dot{\Sigma} = \pi G \Sigma_g^2 \quad (14)$$

The above represents a simple derivation of a Schmidt law, other similar options have been proposed that lead also to Schmidt laws with exponents between 1-2, e.g. Firmani et al. (1996). We now use a characteristic time for the star formation process in the disk $\tau_{sf} = \Sigma_g / \dot{\Sigma}$, that gives an idea of the time a galaxy can support a star formation rate of constant magnitude; if its value is small, the duration of star formation processes will be short, the population presently old and consequently, the galaxy will be red and have a low gas fraction. On the other hand, a galaxy with large τ_{sf} will experience a long star formation duration, and show a young population resulting in bluer colours and a high gas fraction.

From the above relation τ_{sf} becomes

$$\tau_{sf} = \frac{\pi G}{\Sigma_g} = \frac{2\pi^2 G R_d^2}{M_d} \quad (15)$$

Notice that at fixed disk mass (or fixed V_d , through the Tully-Fisher relation), from eq(11) λ will scale with R_d , which translates into a relation between τ_{sf} and λ :

$$\tau_{sf} \propto \lambda^2. \quad (16)$$

In the above, representative values of $\kappa(r)$, $\Omega(r)$, $\Sigma(r)$, $\sigma(r)$ and $\rho_g(r)$ have been assumed, for example, evaluating all variables at $r = R_d$. If one assumes a different star formation scheme from what was used above, equation (16) will change. However, for a variety of similar simple schemes, the proportionality given will be altered only in the change of the exponent, which will remain > 1 . Alternatively, one could start from an empirical Schmidt law of power n , a scaling $\tau_{sf} \propto \lambda^n$ will always result, which does not alter our conclusions provided $n > 1$, a general trait of Schmidt laws found in the literature e.g. Silk (2001).

Large values of λ will correspond to long star formation periods; for this case we expect to have galaxies with young populations and looking relatively blue. Galaxies with low λ will have short star formation periods; for them we will hardly see young stars and they will look red and gas poor. A scatter on this trend will be introduced by variations in total mass, together with a systematic reduction in τ_{sf} in going to larger masses (c.f. equation 15), in accordance with larger average galactic masses found at earlier types.

The ratio of disk scale height to disk scale length, h/R_d , is another measurable characteristic of galaxies which it is easy to show, will also scale with λ . Assuming a thin disk, virial equilibrium in the vertical direction (Binney and Tremaine 1994) yields a relation between h and Σ ,

$$h = \frac{\sigma_g^2}{2\pi G\Sigma}. \quad (17)$$

We use this relation for h to replace the gas velocity dispersion appearing in equation (12) for a combination of h and the surface density. The dependence on Σ is replaced by a dependence on M_d , M_H and λ to get a new expression for the Toomre's stability criterion, which evaluating radial dependences at $r = R_d$ yields,

$$Q^2 = e^{2.5/2} \left(\frac{M}{M_d}\right) \left(\frac{h}{R_d}\right) \lambda \quad (18)$$

With $F = 1/25$, evaluating at $Q = 1$, the stability threshold suggested by self-regulated star formation cycles, the ratio h/R_d is obtained as:

$$\frac{h}{R_d} = \frac{1}{390\lambda}, \quad (19)$$

a simplified version of the result of van der Kruit (1987). For the Galactic value derived above of $\lambda_{MW} = 0.0234$, equation (19) gives $R_d = 9h$, not in conflict with parameters for the Milky Way. For galaxies with large values of λ we expect thin systems, while galaxies with small values of λ will show thick disks, as the observed trend of (h/R_d) decreasing in going from early-type disks to late type galaxies e.g. de Grijs (1998), Yoachim & Dalcanton (2005).

Another important observable characteristic of the morphology of a galaxy, which shows clear trends with Hubble type, is the bulge to disk ratio B/D . From observations it is clear that the central regions of the disk of a galaxy are dynamically "hot", because of the large velocity dispersion present in comparison to the tangential rotation velocity. With this in mind, we introduce a kinematic definition of the bulge (e.g. Hernandez 2000) as the region where the velocity dispersion is comparable to the circular velocity of the disk. The ratio will be given by

$$\frac{B}{D} = \frac{\int_0^a 2\pi\Re\Sigma(\Re)d\Re}{\int_a^\infty 2\pi\Re\Sigma(\Re)d\Re}, \quad (20)$$

with \Re defined as $\Re = r/h$ and a a dimensionless parameter ≥ 1 . The bulge mass is the mass contained from the center of the disk to a distance equal to a multiple of h ; ah , and the disk mass is the remainder. The dependence of the h/R_d ratio is changed for a dependence in λ , using equation (19). The above equation leads to:

$$\frac{B}{D} = \frac{L(e^{a/L} - 1) - a}{L + a} \quad (21)$$

where we have introduced $L = 390\lambda$. We expect to find galaxies with large bulges for low λ values. Of course, other processes which we have not considered, such as all manner of galactic interactions, will result in angular momentum transfer and generally the induction of matter flows towards the bottom of the potential well, i.e. an increase in the B/D ratio. This leads us to expect significant spread.

Also, the analysis of this section implies an increase in values of R_d and a decrease in Σ_0 for more flattened, high λ disks. This could account for the observation of a negative correlation between R_d and Σ_0 found by Kregel et al. (2005). These authors also find through dynamical modeling of galaxies having 2D photometry, that the mass to luminosity ratios of galaxies increase for more flattened (low h/R_d ratios) disks. This last trend appears naturally if we think of flattened disks as coming from high λ values, leading to large R_d and hence galactic disks that extend far out into their dark halos, out to regions where the dominance of the dark component is increasingly obvious. Compounding the above is the fact that volume density of disks scales with $(hR_d^2)^{-1}$, hence since h scales with λ^{-1} and R_d does so with λ^2 , to this level of the analysis, the volume density of the disk will decrease linearly with λ , leading to a decrease in the gravitational potential of the disk. Variations in mass will again introduce scatter into the above trends.

As we have shown in this sub section, in general, galaxies with small values of λ would be expected to be red, have a low gas content, show little present star formation, thick disks and typically large bulge to disk ratios, the defining traits of early spirals. On the other hand, for large values of λ , we expect blue, thin galaxies showing the small bulge to disk ratios of late-type and low surface brightness (LSB) disks. It appears reasonable to expect the observational estimates of λ of eq(11) to show all the trends of the Hubble sequence, indeed, from the point of view of galactic formation scenarios, it is λ what defines a galaxy's type (e.g. Fall & Efstathiou 1980 van der Kruit 1987, Flores et al. 1993, Dalcanton et al. 1997, Hernandez & Gilmore 1998 and van den Bosch 1998).

Notice that this simple model will be valid independently of the formation scenario of a disk galaxy. Whether low values of λ for early spirals are fixed in the remote past as initial conditions, or the result of cancellation of angular momentum due to repeated mergers, equation(11) will still give a reasonable estimate of the value of λ for a disk galaxy at a given time of observation. The model presented in this section isolates the main physical ingredients responsible for the correlations between the galactic observables described. Other more complex and complete models have been presented in the past, which however do not deviate

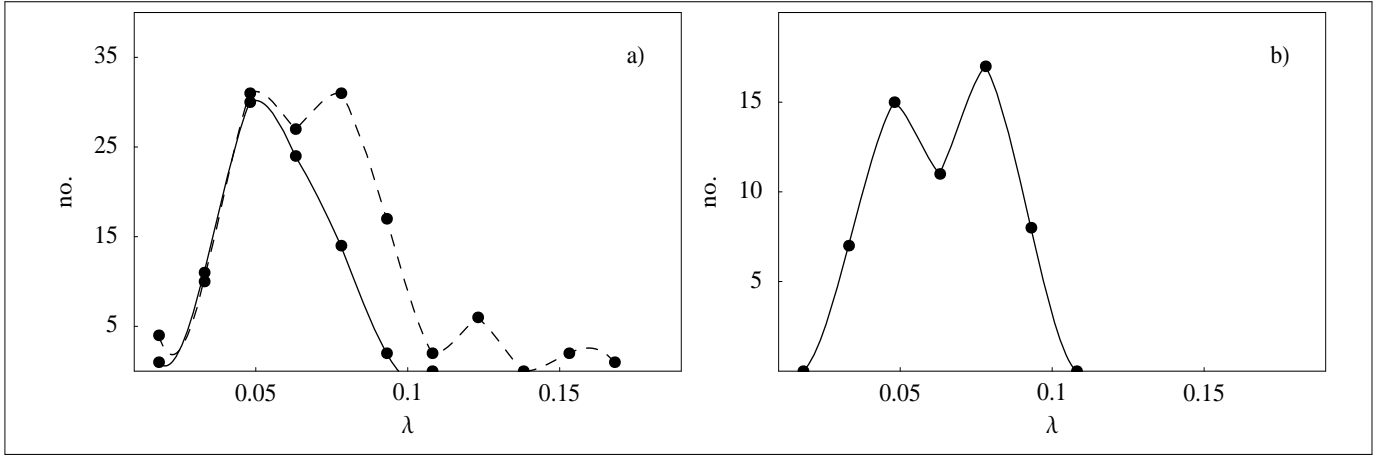


Figure 2.

a) The solid line represents the distribution of values of λ through eq(11) for Sb galaxies in the ASSSG sample, the dashed line gives the equivalent distribution for Sc galaxies. b) Distribution of values of λ for the Sbc galaxies in that same sample. Dots showing the binning.

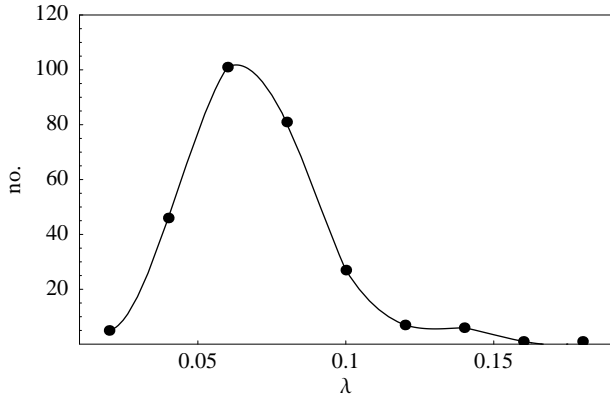


Figure 1. Distribution of values of λ through eq(11) for the complete ASSSG sample, with dots showing the binning

significantly from the basic assumptions of section (2.1), and consequently reach conclusions not drastically different from the ones of section (2.2), if we limit the comparison to only the specific aspects of the problem being treated here. Examples of the above are the analytical schemes of van der Kruit (1987), refined later by Dalcanton et al. (1997), or the more numerical schemes of Fall & Efstathiou (1980), Flores et al. (1993), before the arrival of fuller hydrodynamical and cosmological simulations.

3 OBSERVATIONAL DATA

To compare the relations obtained in the preceding section with observational data of real galaxies we used two samples of galaxies; the Atlas for Structural Studies of Spiral Galaxies (ASSSG) of the Spiral Galaxy data base of Courteau (1996, 1997) and a sample taken from de Grijs (1998) based on the Surface Photometry Catalog of the ESO-Uppsala Galaxies (ESO-LV; Lauberts & Valentijn 1989), and the subsequent re-analysis of these data by Kregel et al. (2002), henceforth dGKK. This last work considers carefully issues related to dust contamination, projection and radial variations in disk scale height. The ASSSG consists of a data

base of 304 late-type spiral galaxies including structural parameters such as rotation velocities and R_d , measured in the r-band. This last point is important, as we require a measure of the extent of the disk mass, and red bands are more sensitive to underlying old stellar populations and are little affected by dust.

From this sample we used the reported disk circular velocity measured at 2.15 disk scale-lengths, the corrected disk scale length, the color term B-R and the ratio of fitted disk light to total measured light for the whole galaxy. This last to estimate B/D ratios. The spectral band used for these measurements was the R band. All the galaxies which show some kind of interaction were suppressed for the analysis, together with spherical and irregular galaxies. One difficulty of using this sample, in connection with our present goals, is the lack of early type spirals. This will make trends with Hubble type appear harder to detect, as it is often between the Sa and the latter types that the largest changes occur. However, the uniform treatment of the data, the large sample and the long observational wavelengths make the ASSSG sample worthwhile. If some trends can be seen even in the absence of Sa galaxies, as it is indeed the case, it is to be expected that their inclusion would only strengthen further our conclusions.

The dGKK sample consists of 33 edge-on galaxies from which we used the I-band exponential scale height and exponential scale length and the maximum rotational velocity. Again, it is the red wavelength of observation that makes this particular sample relevant to our analysis.

As mentioned in the preceding section, we expect a correlation between the λ parameter and the Hubble type, since the analysis of section 2 leads one to suspect that it is this what primarily determines the properties of the galaxy which are taken into account for its classification. In figure 1 we present the distribution of the ASSSG sample as a function of λ , estimated through eq(11). For the entire sample, the mean value is $\langle \lambda \rangle = 0.0645$. We see an approximately Gaussian shape, with a considerable extension towards the larger values of λ . We do not explore the details of this distribution further, as the ASSSG sample is not intended to

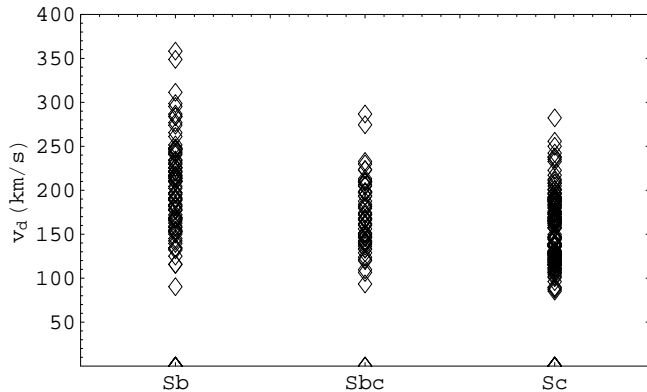


Figure 3. Hubble type as a function of the circular velocity for the galaxies in the ASSSG sample.

be complete or statistically unbiased in any sense. However, use of eq(11) in one such sample should prove useful in obtaining an empirical distribution of λ parameters, to compare for example, against predictions from cosmological models. These models yield theoretical distributions for galactic values of λ resulting from tidal interactions of the material accreting onto a protogalaxy and global surrounding dark matter tidal fields, which are sensitive to cosmological parameters such as Ω_Λ and the details of the initial fluctuation spectrum (e.g. Warren et al. 1992, Cole & Lacey 1996, Catelan & Theuns 1996 and Lemson & Kauffmann 1999). The above parameters could in principle then be constrained through empirical inferences of the present day distribution of λ inferred through equation (11) and a large unbiased sample of galaxies.

Second, we divide the ASSSG sample by Hubble type into three groups; Sb, Sbc and Sc. The result is shown in figure 2, where the continuous curve in panel a) shows the distribution of values of λ for the Sb's and the dashed curve for the Sc's. We see that as expected, Sc's are characterized by larger values of λ , although significant overlap occurs. Panel b) gives the λ distribution for the subclass Sbc's, by comparing to panel a) it is interesting that this class appears as a superposition of the previous two classes, with the exception of the tail towards large λ s seen in the Sc sample. This last point highlights the difficulty in making detailed distinctions among subclasses in the Hubble sequence, and agrees with the conclusions of Ellis et al. (2005), who analyze and classify automatically through a variety of elaborate statistical analysis on many galactic parameters a large sample of galaxies, and conclude that only two definitive classes are naturally suggested by the data, late and early spirals.

In general, the bulk of a galactic population moves to larger values of λ for later types, the mean value for each group is: $\langle \lambda \rangle_{Sb} = 0.0574$, $\langle \lambda \rangle_{Sbc} = 0.0649$, $\langle \lambda \rangle_{Sc} = 0.0689$.

Next we analyze and compare the statistical distributions of V_d as functions of Hubble type and λ , also for the ASSSG. In figure 3 we present the distribution of galactic rotation velocities V_d with morphological type. Earlier types present a wide dispersion of velocities, which diminishes slightly for the later types, where lower mean values are found. For this analysis we obtained mean values for every sub-sample; $\langle v \rangle_{Sb} = 205.41 \text{ km/s}$, $\langle v \rangle_{Sbc} = 172.42 \text{ km/s}$ and $\langle v \rangle_{Sc} = 155.95 \text{ km/s}$, a monotonic trend is clear, al-

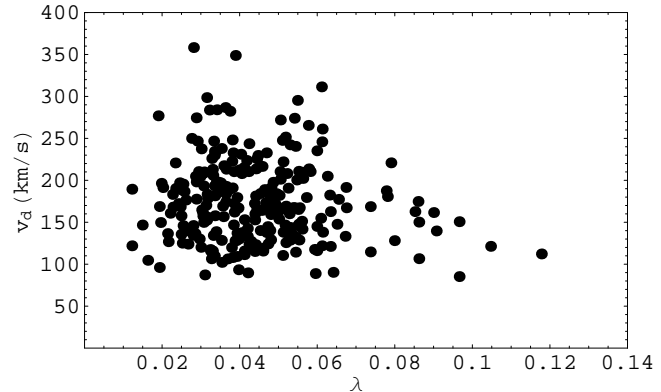


Figure 4. Values of the circular velocity plotted against λ through eq(11) for the galaxies in the ASSSG sample.

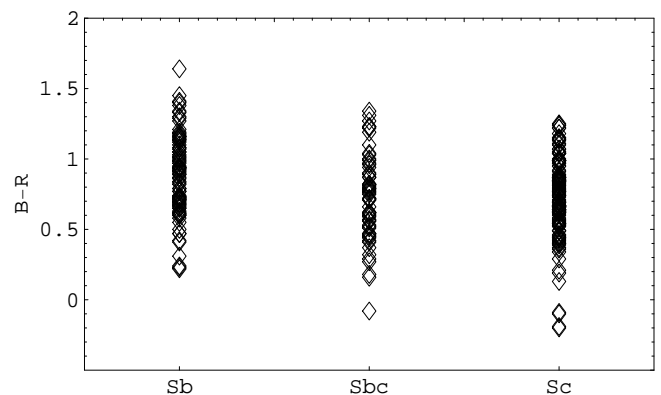


Figure 5. Relation between the Hubble type and the B-R color term, for the galaxies in the ASSSG sample.

though very significant overlap is present. This result is well known, and reflect the similar trend of decreasing total luminosities with Type, e.g. Roberts & Haynes (1994), Ellis et al. (2005).

Figure 4 gives a plot of V_d vs. λ for the galaxies appearing in figure 3. We see that despite considerable dispersion and overlap, galaxies with large values of λ are restricted to the lower values of V_d , while at low values of λ a much wider range of V_d is present. The mean V_d at each λ decreases with λ , as is seen when plotting against Hubble type in figure 3.

An important measurable parameter for the classification of a galaxy is its color, giving information on the evolutionary state of the stellar population. One of the clearest trends seen along the Hubble sequence is precisely the shift to bluer colours when going towards the later types (e.g. Roberts & Haynes 1994, Park & Choi 2005). The ASSSG sample shows this expected relation clearly in figure 5, where we plot B-R colour for the different types.

In section 2, we proposed a relation between λ and the color of a galaxy supported by the idea of the existence of a characteristic timescale for the star formation process, which should increase with λ . In order to examine the validity of our statement we present the relation of these two parameters for the ASSSG sample in figure 6. It is clear that the sample follows a marked tendency, the B-R term decreases with λ , which is in agreement with our predictions. The agreement of this trend with the equivalent one seen for Hubble types reinforces the idea that the single most impor-

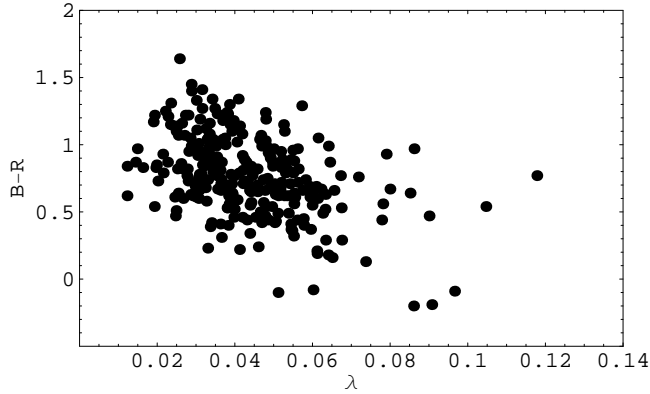


Figure 6. Values of the B-R color term plotted against λ through eq(11) for all the galaxies in the ASSSG sample.

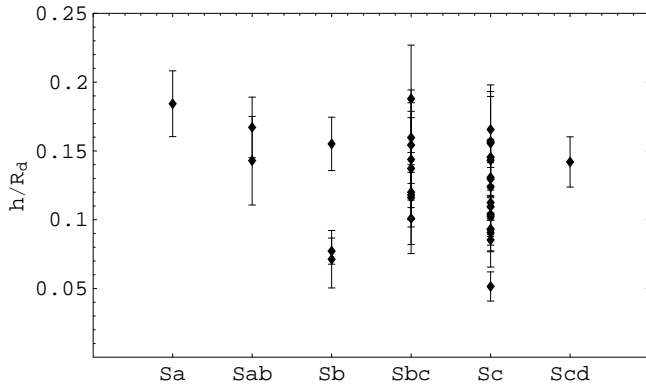


Figure 7. h/R_d ratios for galaxies according to their Hubble type, for galaxies in the dGKK sample.

tant galactic parameter which is varying along the Hubble sequence is precisely λ .

The analysis of the distribution of h/R_d ratios was made with the dGKK sample. It contains galaxies with more morphological types; from Sa to Scd galaxies. This spread of types allow us to see clearly if there is any kind of tendency regarding the h/R_d ratio and the Hubble types. Figure 7 shows early galaxies presenting varied values for the h/R_d ratio, although the means show a clear diminishing trend in going to latter types, very similar to what was seen for V_d and colour. Late type galaxies at the Sc end clearly show on average much thinner disks than the earlier types, as confirmed by several authors over the last few years e.g. Yoachim & Dalcanton (2005). It is interesting to note that in the re-analysis of the de Grijs (1998) data by Kregel et al. (2002) not only do the values of R_d and h change, but perhaps surprisingly, the Hubble types of the galaxies are significantly shifted around, sometimes by more than 1 subtype. This last point highlights again the subjective nature of “type” classification schemes for galaxies.

The complementary plot to figure 7 is given in figure 8, where instead of presenting h/R_d vs λ , we use a logarithmic plot to better detect the presence of a relation between these two parameters of the type the dimensional analysis of section 2 leads us to expect, equation(19). The line drawn in figure 8 is the best fit straight line for the sample, having a slope of -0.4 ± 0.9 , not at odds with value of -1 predicted by the simple model. The expectations of the model are seen

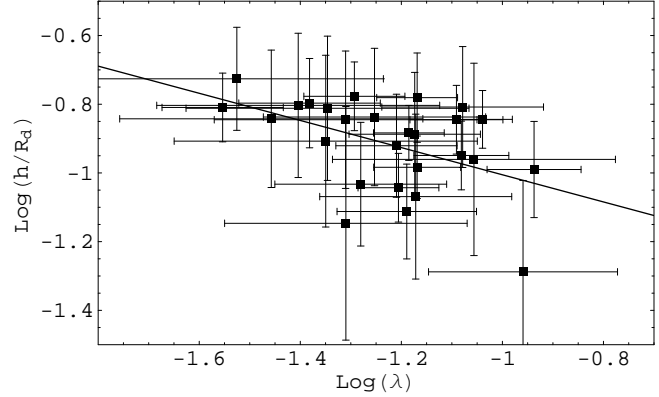


Figure 8. Logarithmic plot of the relation between λ and h/R_d , for galaxies in the dGKK sample, the solid line shows a linear fit to the data, yielding a slope of -0.4 ± 0.9 .

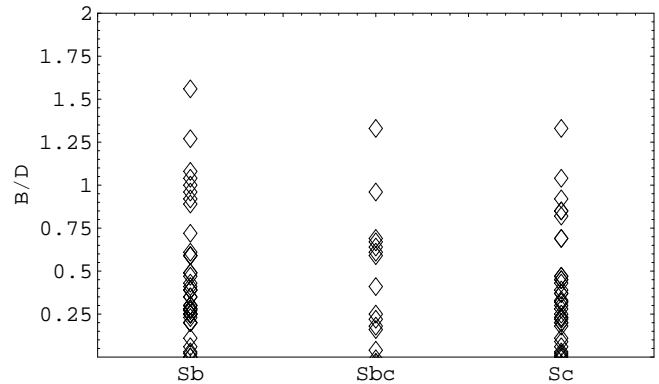


Figure 9. B/D ratios for galaxies classified by their Hubble type, for the ASSSG sample.

to be generally borne out by the data, albeit the large errors present.

The last galactic property which we analyze is the bulge to disk ratio B/D . For this we return to the ASSSG sample, and attempt an estimate of this parameter from the reported total light, and the reported extrapolation for a total disk light coming from the iterpolated central disk brightness and measured disk scale length values, by assuming that the total measured light is the sum of the disk light and the light coming from the bulge. This is of course not ideal, as for example, truncated disks will give artificially large values of the B/D ratio. This and other effect however, will affect all the galaxies of the sample in the same way. Therefore, the error is of the same order of magnitude for each and it allows us to look for and compare trends against both Hubble type and λ , although the actual values of B/D ratios might be off, and the dispersion artificially broadened.

Figure 9 gives these B/D ratios against Hubble type, the extent of values found for each class is comparable, but the means show a very clear trend, with Sc’ clustering at low values of B/D . This trend is again well known, and in fact, small bulges are one of the defining characteristics of late type galaxies.

The final plot of this section, figure 10, gives the same values of the B/D ratio of figure 9, but plotted this time against the value of λ derived for each galaxy in the ASSSG sample through eq(11). We again see something very similar

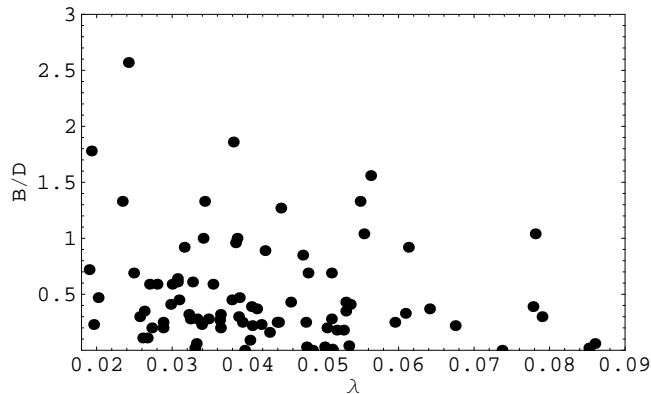


Figure 10. PLOT of B/D ratios for galaxies in the ASSSG sample, as a function of their inferred values of λ from eq(11).

to what the corresponding 'type' figure shows. Indeed, all the galactic properties examined show very similar trends, large dispersions which drop towards later types, with means that show distinctive and very similar decreasing trends with either type or λ . The close equivalence of trends against Hubble type and λ strongly supports the idea that a combination of spatial extent (through R_d) and dynamics (through V_d) given by the dimensionless λ parameter of eq(11) most closely yields the monotonically changing physical parameter of a galaxy responsible for its Hubble type. All the trends seen against λ are noisy, but not more so than the corresponding ones against Hubble type, and often better, with the advantages of λ being objective, readily obtainable through the simple relation of eq(11) and representing a dimensionless parameter having a direct physical interpretation.

4 DISCUSSION

In this final section we discuss some aspects of the ideas proposed, and include a small comparison of equation(11) against CDM galactic computer formation codes. A physical model simplified to the extreme, as what was presented in section 2, will only be of any use if the few ingredients which remain manage to capture the fundamental physical processes responsible for the aspects of the problem one is interested in. For example, in a strong explosion, the first phases are completely determined by the energy released and the density of the medium where the explosion takes place, these two numbers and a trivial dimensional analysis suffice to obtain the Sedov-Taylor solution, which is an accurate description of the problem. Indeed, complex hydrodynamical computer codes tracing the energetics and dynamics of shocks and explosions are often tested and calibrated in their myriad numerical details against such a simplistic analytic solution.

We must now check our estimate of λ in cases where this parameter is in fact known, galaxy formation simulations where λ acts as an input parameter. We use results from two groups, the Firmani et. al (1998) approach, models calculated in connection with a study of star formation in disk galaxies applied to the Milky Way (Hernandez et al. 2001), and the models published by van den Bosch (2000). A very brief description of such models is included below.

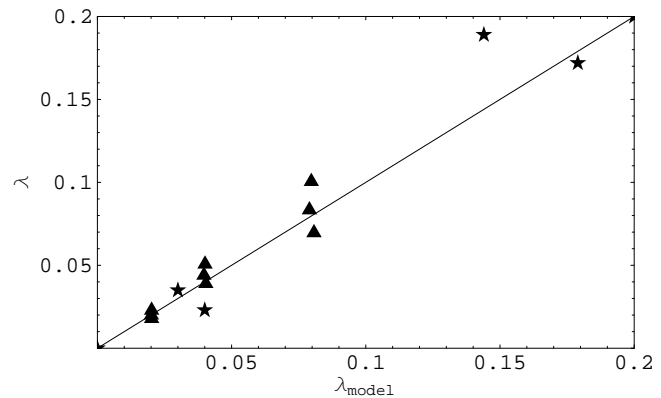


Figure 11. A comparison of the input value of λ in a series of cosmological CDM galactic evolution scenarios, λ_{model} , and λ calculated on the final result of the given simulations through eq(11). The triangles are models from Hernandez et al. (2001) and stars from van den Bosch (2000).

The first of these models includes a very wide range of physics, initial conditions are supplied by an statistical sampling of a cosmological primordial fluctuation spectrum, giving a mass aggregation history of gas and dark matter. No Tully-Fisher type of relation is assumed *a priori*, indeed, this codes attempt to recover such a relation as a final result of the physics included. A fixed value of λ is assumed for the infalling material which settles into a disk in centrifugal equilibrium and differential rotation, viscous friction results in radial flows of matter and angular momentum. The redistribution of mass affects the rotation curve in a self-consistent way, through a Poisson equation including the disk self gravity and a dark halo which responds to mass redistributions through an adiabatic contraction. The star formation is followed in detail, with an energy balance cycle of the type discussed in section 2 being introduced.

A simple population synthesis code then traces the luminosities and colours of the various stellar populations at all radii and times. The details of the van den Bosch (2000) models vary in numerical approaches, resolution, time step issues and the level of approximation and inclusion of the many different physical aspects of the complicated problem. Figure 11 shows the λ_{model} values given as input by the above authors to their detailed formation codes, with the y-axis showing λ from equation (11) applied to the final results of the code evolution which followed the model for ~ 13 Gyr. Stars for the van den Bosch (2000) results and triangles for the Hernandez et al.(2001) models.

It is interesting that the particular features of a galactic formation scenario which we are interested in treating here, λ , final resulting R_d and flat rotation region V_d , are evidently very well modeled by the trivial physics that went into eq(11), across the more than 2.5 orders of magnitude covered by the masses in the modeled galaxies. This can be understood by considering that eq(11) is the result of two fundamental hypothesis: I) an exponentially decreasing surface density profile for the disk, and II) a dominant dark halo responsible for a flat rotation curve linked to the disk through a Tully-Fisher relation. Whenever these two conditions are met, as is the case for the final state of all published modeled galaxies and real observed systems, basic physics strongly constrains results to lie not far from equation (11).

For example, Kregel et al. (2005) clearly identifies the good agreement between the models of Dalcanton et al. (1997) and their dynamical and photometric data as an unavoidable corollary of the two hypothesis listed above within an approximately constant Q parameter, irrespective of the actual galactic formation scenario.

This of course, is not to say that eq(11) replaces a detailed galactic formation scenario, which is really the only way of treating the time evolution of the problem, and to arrive at the physical origin of many of the well known galactic features which were introduced as empirical facts into the development leading to eq(11). To mention only two such problems, the origin of Tully-Fisher relation can be traced through CDM galactic formation simulations (e.g. Avila-Reese et al. 1998, Steinmetz & Navarro 1999, Navarro & Steinmetz 2000), as can the causes of the observed exponential density surface brightness profiles of galaxies (e.g. Saio & Yoshii 1990, Struck-Marcell 1991, Firmani et al. 1996, Silk 2001, Zhang 2000, Bell 2002).

To conclude, we have presented an easily applicable way of estimating the λ parameter, a theorist's favourite descriptor of a galaxy type, for any real observed disk galaxy. We have shown that four determinant galactic properties crucial in the subjective assignment of a Hubble type to an observed disk system correlate well with the introduced λ parameter, in ways very similar to what is seen when comparing against the classical Hubble type for late type galaxies. We suggest that any other dimensionless galactic parameter for late type disks will also show analogous trends with λ of eq(11), as would be expected from Buckingham's theorem of dimensional analysis (Sedov 1993). The well defined and objective nature of the dimensionless λ parameter, both in simulations and in real galaxies through eq(11), should make it a useful tool in comparing the output of numerical galactic formation scenarios and real galaxy samples.

ACKNOWLEDGMENTS

The authors wish to thank Juliane Dalcanton for her help during the preparation of the manuscript and the input of an anonymous referee which improved the final version. The work of X. Hernandez was partly supported by DGAPA-UNAM grant No IN117803-3 and CONACYT grants 42809/A-1 and 42748. The work of B. Cervantes-Sodi is supported by a CONACYT scholarship.

REFERENCES

- Adams A., Woolley, A., 1994, VA, 38, 273
 Abraham R. G., Tanvir N. R., Santiago B. X., Ellis R. S., Glazebrook K., van den Bergh S., 1996, MNRAS, 279, L47
 Abraham R. G., Valdes F., Yee H. K. C., van den Bergh S., 1994, ApJ, 432, 75
 Avila-Reese V., Firmani C., Hernandez X., 1998, ApJ, 505, 37
 Bell E. F., 2002, ApJ, 581, 1013
 Binney J., Tremaine S., 1987, Galactic Dynamics (Princeton: Princeton Univ. Press)
 Brosche, P., 1973, A&A, 23, 259
 Catelan P., Theuns T., 1996, MNRAS, 282, 455
 Cole S., Lacey C., 1996, MNRAS, 281, 716
 Connolly A. J., Szalay A. S., Bershady M. A., Kinney A. L., Calzetti D., 1995, AJ, 110, 1071
 Conselice C., 2003, ApJS, 147, 1
 Courteau S., 1996, ApJS, 103, 363
 Courteau S., 1997, AJ, 114, 2402
 Dalcanton J. J., Spergel D. N., Summers F. J., 1997, ApJ, 482, 659
 de Grijs R., 1998, MNRAS, 299, 595
 de Vaucouleurs G., 1959, Handbuch der Physik, 53, 275
 Dopita M. A., Ryder S. D., 1994, ApJ, 430, 163
 Ellis S. C., Driver S. P., Allen P. D., Liske J., Bland-Hawthorn J., De Propriis R., 2005, MNRAS, 363, 1257
 Fall S. M., Efstathiou G., 1980, MNRAS, 193, 189
 Ferguson A. M. N., Clarke C. J., 2001, MNRAS, 325, 781
 Frenk C. S., White S. D. M., Efstathiou G., Davis M., 1985, Nature, 317, 595
 Frenk C. S., White S. D. M., Davis M., Efstathiou G., 1988, ApJ, 327, 507
 Flores R., Primack J. R., Blumenthal G. R., Faber S. M., 1993, ApJ, 412, 443
 Firmani C., Hernandez X., Gallagher J., 1996, A&A, 308, 403
 Firmani C., Avila-Reese V., Hernandez X., 1998, ApJ, 505, 37
 Graham A. W., 2001, AJ, 121, 820
 Grosbol P., Patsis P. A., Pomoei E., 2004, A&A, 423, 849
 Gurovich S., McGaugh S. S., Freeman K. C., Jerjen H., Staveley-Smith L., De Blok W. J. G., 2004, PASA, 21, 412
 Hernandez X., Avila-Reese, V., Firmani, C., 2001, MNRAS, 327, 329
 Hernandez X., 2000, in ASP Conf. Series, 215, Cosmic Evolution and Galaxy Formation: Structure, Interactions, and Feedback, eds. Franco J., Terlevich E., Lopez-Cruz O., Aretxaga I., 113
 Hernandez X., Gilmore G., 1998, MNRAS, 294, 595
 Hubble E. P., 1926, ApJ, 64, 321
 Hubble E. P., 1936, Realm of the Nebulae (New Haven: Yale Univ. Press)
 Kelly B. C., McKay T. A., 2004, AJ, 127, 625
 Kregel M., van der Kruit P. C., de Grijs R., 2002, MNRAS, 334, 646
 Kregel M., van der Kruit P. C., Freeman K. C., 2005, MNRAS, 358, 503
 Klypin A., Zhao H., Somerville R. S., 2002, ApJ, 573, 597
 Koeppen J., Theis C., Hensler G., 1995, A&A, 296, 99
 Kormendy J., 1979, ApJ, 227, 714
 Kuchinski L. E., et al., 2000, ApJS, 131, 441
 Labbe I. et al., 2003, ApJ, 591, L95
 Lauberts A., Valentijn E. A., 1989, The Surface Photometry Catalogue of the ESO-Upssala Galaxies. ESO (ESO-LV)
 Lemson G., Kauffmann G., 1999, MNRAS, 302, 111
 Lotz J. M., Primack J., Madau P., 2004, AJ, 128, 163
 Ma J., 2002, A&A, 388, 389
 Maller A. H., Dekel A., Somerville R., 2002, MNRAS, 329, 423
 Mo H. J., Mao S., White S. D. M., 1998, MNRAS, 295, 319
 Naab T., Ostriker J. P., 2005, MNRAS, in press (astro-ph/0505594)
 Naim A., Ratnatunga K. U., Griffiths R. E., 1997, ApJ, 476, 510
 Navarro J. F., Steinmetz M., 2000, ApJ, 538, 477
 Pahre M. A., Ashby M. L. N., Fazio G. G., Willner S. P., 2004, ApJS, 154, 235
 Park C., Choi Y., 2005, ApJ, 635, 29
 Peebles P. J. E., 1969, ApJ, 155, 393
 Roberts M. S., Haynes M. P., 1994, ARA&A, 32, 115
 Sandage A., 1961, The Hubble Atlas of Galaxies (Washington D.C.: Carnegie Institution of Washington)
 Sandage A., Freeman K. C., Stokes N. R., 1970, ApJ, 160, 831
 Saio H., Yoshii Y., 1990, ApJ, 363, 40
 Sedov L. I., 1993, Similarity and Dimensional Methods in Mechanics, 10th edn. (CRC Press)
 Schade D., Lilly S. J., Crampton D., Hammer F., LeFevre O., Tresse L., 1995, ApJ, 451, L1
 Silk J., 2001, MNRAS, 324, 313

- Somerville R. S., Primack J. R., 1999, MNRAS, 310, 1087
Steinmetz M., Navarro J. F., 1999, ApJ., 513, 555
Struck-Marcell C., 1991, ApJ, 368, 348
Takamiya M., 1999, ApJS, 122, 109
Tonini C., Lapi A., Shankar F., Salucci P., 2005, astro-ph/0510577
Toomre A., 1964, ApJ, 139, 1217
van den Bosch F. C., 1998, ApJ, 507, 601
van den Bosch F. C., Dalcanton J. J., 2000, ApJ, 534, 146
van der Kruit, P. C., 1987, A&A, 173, 59
Warren M. S., Quinn P. J., Salmon J. K., Zurek W. H., 1992, ApJ, 399, 405
Wilkinson M. I., Evans N. W., 1999, MNRAS, 310, 645
White S. D. M., Frenk C. S., 1991, ApJ., 379, 52
Yoachim P., Dalcanton J. J., 2005, AJ, in press (astro-ph/0508460)
Zaritsky D., Zabludoff A. I., Willick J. A., AJ, 1995, 110, 1602
Zhang B., Wyse R. F. G., 2000, MNRAS, 313, 310